Diamond nitrogen-vacancy centres spin-state-based quantum sensor using a compact broadband antenna

Cui, Mingming; Shen, Fazhong; Qiao, Yingying; Du, Guanxiang; Zhuo, Xiang; Zang, Jiawei; Zhang, Zhenyuan; Wang, Yi; Li, Lei; Gao, Yang

DOI:
10.1049/ell2.12649

Citation for published version (Harvard):
Cui, M, Shen, F, Qiao, Y, Du, G, Zhuo, X, Zang, J, Zhang, Z, Wang, Y, Li, L & Gao, Y 2022, 'Diamond nitrogen-vacancy centres spin-state-based quantum sensor using a compact broadband antenna', *Electronics Letters*, vol. 58, no. 24, pp. 893-895. https://doi.org/10.1049/ell2.12649

Diamond nitrogen-vacancy centres spin-state-based quantum sensor using a compact broadband antenna

Mingming Cui,[1] Fazhong Shen,[1] Yingying Qiao,[1] Guanxiang Du,[2] Xiang Zhuo,[2] Jiawei Zang,[3] Zhenyuan Zhang,[4] Yi Wang,[5] Lei Li,[1,✉] and Yang Gao[1,✉]

[1]*Zhengzhou University, Zhengzhou City, China*

[2]*Nanjing University of Posts and Telecommunications, Nanjing City, China*

[3]*China Academy of Information and Communications Technology, Beijing, China*

[4]*Southern University of Science and Technology, Shenzhen, China*

[5]*University of Birmingham, Birmingham, UK*

✉Email: gaoyang678@outlook.com, lilei@zzu.edu.cn

This paper presents a compact broadband antenna that is used in the spin-state-based magnetic field quantum sensor. In the diamond nitrogen-vacancy (NV) centre system, the qubit resonance is excited by the microwave signal, and the frequency shift is proportional to the external magnetic field strength. Conventional narrow-band antennas or single resonators are not able to match the resonance frequency of the NV centre over a wide bandwidth, resulting in degraded sensitivity and dynamic range of the sensor. Here, the authors designed a compact broadband antenna, which achieves a fractional bandwidth of 71.43% at the Zeeman splitting frequency of 2.87 GHz. With the introduced slot structure on the antenna, a higher microwave near field strength can also be achieved, which improves the magnetic field sensitivity and dynamic range. By applying our design antenna, the experimental results indicate that the NV-based quantum sensor achieves a sensitivity of 3.07 μT/Hz$^{1/2}$ and a dynamic range up to 44.9 dB, which are both greatly improved compared to sensor that uses a conventional antenna.

Introduction: The diamond nitrogen-vacancy (NV) centre has become an excellent quantum sensor for measuring magnetic field, due to its high-resolution and non-invasive detection [1]. Its structure (Figure 1a) is that one carbon atom in diamond is replaced by a nitrogen atom, and another adjacent carbon atom is missing. Under the excitation of green laser and microwave field, the qubit resonance [3] of the NV centre can be obtained by receiving the optically detected fluorescence generated by the electron spin transition. The Zeeman splitting [1] can also be observed from the fluorescence spectrum, which magnetic field can be measured (Figure 1b). This usually used the optically detected magnetic resonance (ODMR) [3] method for the diamond NV centres-based magnetic field sensor.

Currently, microwave resonators [2], patch antennas [3], coplanar waveguide (CPW) [4], or copper wires [5] are usually used as the microwave delivery and radiation components in the sensing system. However, these microwave components suffer narrow operating bandwidths and low radiation efficiency [6]. Moreover, when the external magnetic field varies, the qubit resonant centre frequency of the NV colour centre shifts, and thus a narrow frequency band device would cause mismatch between the microwave source and the NV colour centre. This decreases the microwave power exerted on the NV centre, reducing fluorescence contrast and sensitivity, or even making the sensor fail to detect. Although there are resonators with variable centre frequency [7] and uniform microwave field distribution [8], they still have the disadvantages of poor frequency matching accuracy, complex circuits, and narrow operating bandwidth.

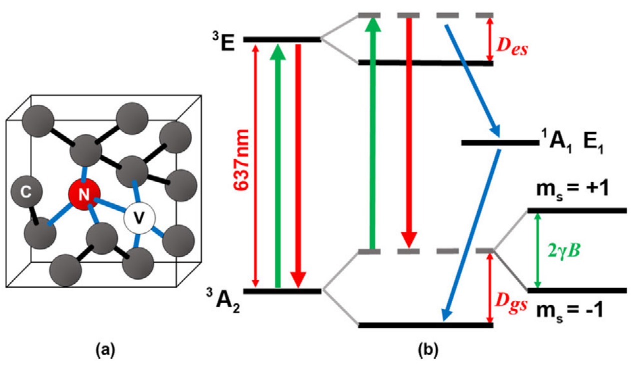

Fig. 1 *(a) Structure of NV colour centre in diamond. (b) Energy levels of the NV centre. NV, nitrogen-vacancy.*

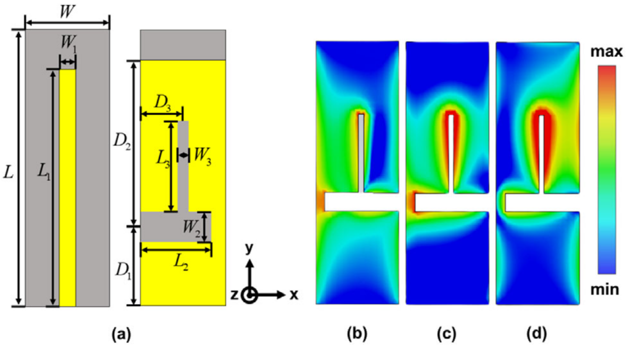

Fig. 2 *(a) is the front and background view of the broadband antenna. The yellow parts are the feeder line and ground plane, covered with copper, (b) (c), and (d) are the current distribution of antenna at 2.0 , 3.0, and 4.0 GHz.*

Table 1. Filtering antenna dimensions

Parameters	Values (mm)	Parameters	Values (mm)	Parameters	Values (mm)
L	44.55	D_1	16.12	L_3	12.32
W	13.76	D_2	25.25	W_3	0.86
L_1	29.49	L_2	12.32	D_3	6.26
W_1	1.71	W_2	2.91		

Herein, a broadband antenna is designed. The dual-mode resonant broadband response can be achieved using a slot structure on the microstrip, which allows for an improved magnetic sensing range up to 9.43 × 10^{-2} T, corresponding to the dynamic range of 44.9 dB. Additionally, due to the slot structure, a strong electromagnetic intensity can also be achieved over a square-millimetre area, resulting in a significantly improved sensitivity of the quantum sensor.

Broadband antenna design: There are two resonant modes used in the antenna. The dipole-like mode generates a low-frequency resonance point and is determined by the ground plane length. The open-slot mode generates two high resonance points, and the highest resonance frequency is determined by the vertical slot length [9]. The resonant frequencies f_d and f_o can be estimated by

$$f_d \approx \frac{c}{2L_g\sqrt{\varepsilon_e}},\ f_o \approx \frac{c}{4L_s\sqrt{\varepsilon_e}} \tag{1}$$

where L_g is the length of the ground plane, L_s is the length of the vertical slot, ε_e is (when $W_l > h$)

$$\varepsilon_e = \frac{\varepsilon+1}{2} + \frac{\varepsilon-1}{2}\left[1+12\frac{h}{W_l}\right]^{-1/2} \tag{2}$$

where ε is the dielectric constant, h is the thickness of the media substrate, and W_l is the width of the feeder.

The structure of the broadband antenna is shown in Figure 2a. According Equations (1) to (2), the original dimensions of the antenna can be calculated. After optimized geometries of the antenna are given in Table 1, the substrate used is RT/5880 with a dielectric constant ε of 2.2 and a thickness h of 1.575 mm.

To verify the resonant mode of the antenna, we simulate the current distribution on the antenna surface at the three resonant points. The current is distributed at the side of the ground plane at 2.0 GHz (Figure 2b),

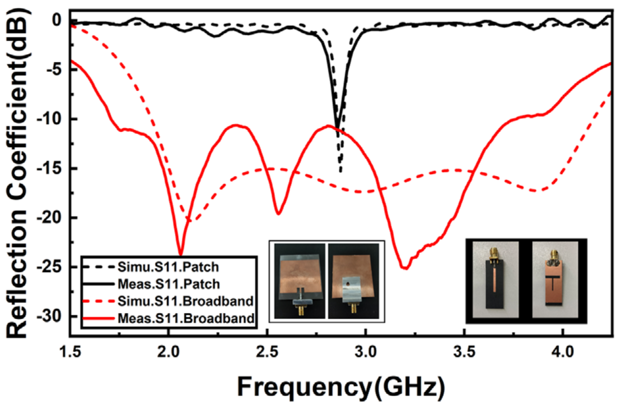

Fig. 3 *Simulated and measured S11 of patch antenna and broadband antenna*

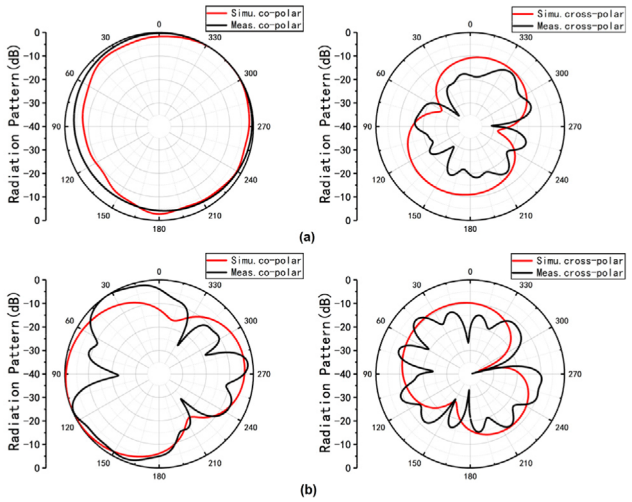

Fig. 4 *Simulated and measured radiation pattern of broadband antenna at 2.87 GHz with (a) H-plane (XOZ) and (b) E-plane (YOZ)*

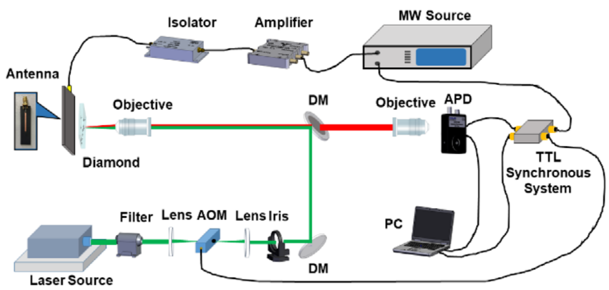

Fig. 5 *Schematic diagram of the experimental system*

while the current is distributed near the edge of the slot at 3.0 and 4.0 GHz (Figures 2c, 2d). The distribution of the surface current verifies the existence of two resonant modes.

To make a comparison, the conventional patch antenna that is usually used in the diamond quantum sensor is also manufactured. The simulated and measured S_{11} of patch antenna and broadband antenna are shown in Figure 3. The bandwidth of the antenna is 1.71 to 3.76 GHz. The radiation pattern of broadband antenna at 2.87-GHz Zeeman splitting frequency is shown in Figure 4.

NV-centres-based quantum sensing system using the broadband antenna: The experimental system setup is shown in Figure 5. A 532-nm wavelength laser is used to pump the diamond NV centres from the $^3A_2$ ground state to the ^3E excited state. The ground state of NV centres includes a triplet $|m_s = 0, \pm 1\rangle$ state, which includes $|m_s = \pm 1\rangle$ and $|m_s = 0\rangle$ states. There are radiative transition and non-radiative transition from the ^3E excited state to the $^3A_2$ ground state. The $|m_s = \pm 1\rangle$ states of NV centres contain a non-radiative transition, while the $|m_s = 0\rangle$ states of NV

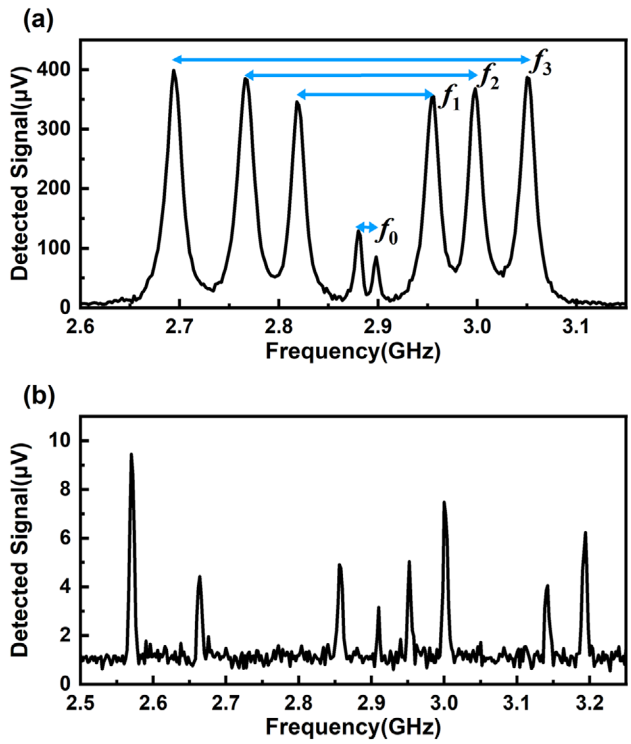

Fig. 6 *ODMR curves of (a) broadband antenna and (b) patch antenna measured under the same magnetic field. ODMR, the optically detected magnetic resonance.*

centres perform a radiative transition. For the radiative transition, the NV centres can emit 600-nm red fluorescence, which can be collected by the photodiode and readout.

The measured ODMR spectrum curve is shown in Figure 6a, where Zeeman splitting can be clearly observed. As a comparison, the measured ODMR spectrum of the patch antenna, which is conventionally used in previous studies, is shown in Figure 6b. The magnetic field components projected on the NV axes corresponding to Δf_i $(i = 0, 1, 2, 3)$ can be calculated by

$$B_i = \frac{\Delta f_i}{\gamma_e} \tag{3}$$

where γ_e is the gyromagnetic ratio, 28 GHz/T.

The antenna magnetic measurement sensitivity can be calculated by [10]

$$\eta = \frac{\sigma}{\gamma_e m} \tag{4}$$

where σ (unit: V/Hz$^{1/2}$) is the measured noise floor, given by 2.62 μV/Hz$^{1/2}$ (broadband antenna) and 0.65 μV/Hz$^{1/2}$ (patch antenna). m (unit: V/MHz) is the maximum slope of the ODMR curve given by 3.05 μV/MHz (broadband) and 1.54 μV/MHz (patch). Accordingly, the sensitivity of magnetic sensor with broadband antenna is 15.04 μT/Hz$^{1/2}$, which improves about five times of the conventional patch antenna of 3.07 μT/Hz$^{1/2}$. A comparison of NV-based magnetic field sensors is presented in Table 2. Compared with [7, 8, 11], our proposed sensor also has a great improvement in operating bandwidth, corresponding to a maximum detection dynamic range of 44.9 dB.

Conclusion: This article reports a novel broadband antenna that is used for diamond NV centre-based magnetic field quantum sensor. The sensitivity and the dynamic range are improved due to the introduced antenna. This broadband antenna or other microwave circuits allow us to envision potential low-cost, flexible, and practical quantum-based sensing or other applications.

Table 2. Comparison of NV-based magnetic field sensors

Ref.	**Microwave delivery**	**Operating bandwidth**	**Sensitivity**	**Maximum detection range**	**Dynamic range**
This	Broadband antenna	2.64 GHz	3.07 μT/Hz$^{1/2}$	9.43×10^{-2} T	44.9 dB
Work	Patch antenna	0.13 GHz	15.04 μT/Hz$^{1/2}$	4.64×10^{-3} T	24.9 dB
[7]	Freq-tunable resonator	0.6 GHz	N/A	3×10^{-3} T	7.8 dB
[8]	Split-ring resonator	0.04 GHz	$\sim$fT/Hz$^{1/2}$	5.59×10^{-4} T	0.7 dB
[11]	Open-loop ring filtering antenna	0.73 GHz	8.52 μT/Hz$^{1/2}$	15.93×10^{-3}T	32.73 dB

Author Contributions: Mingming Cui: Data curation; Investigation; Software; Visualization; Writing – original draft. Fazhong Shen: Project administration; Resources; Supervision; Writing – review & editing. Yingying Qiao: Project administration; Supervision; Writing – review & editing. Guanxiang Du: Resources; Writing – review & editing. Xiang Zhuo: Resources; Validation. Jiawei Zang: Resources; Validation; Writing – review & editing. Zhenyuan Zhang: Project administration; Supervision. Yi Wang: Supervision; Writing – review & editing. Lei Li: Funding acquisition; Project administration; Supervision; Writing – review & editing. Yang Gao: Conceptualization; Funding acquisition; Methodology; Supervision; Writing – review & editing.

Acknowledgements: This work was supported by the National Natural Science Foundation of China (NO. 62105294) and the National Key Scientific Instrument and Equipment Development Project of China (NO. 6202780147).

Conflict of Interest: The authors have no conflict of interest to declare.

Data availability statement: Research data are not shared.

Received: *21 July 2022* Accepted: *3 October 2022*
doi: 10.1049/ell2.12649

References

1 Maze, J.R. et al.: Nanoscale magnetic sensing with an individual electronic spin in diamond. *Nature* **455**(7213), 644–647 (2008)

2 Yang, X., Zhang, N., Yuan, H., Bian, G., Fan, P., Li, M.: Microstrip-line resonator with broadband, circularly polarized, uniform microwave field for nitrogen vacancy center ensembles in diamond. *Aip. Adv.* **9**(7), (2019) Art. no. 075213

3 Yang, B. et al.: Using diamond quantum magnetometer to characterize near-field distribution of patch antenna. *IEEE Trans. Microw. Theory Tech.* **67**(6), 2451–2460 (2019)

4 Ayissi Eyebe, G., Sama, N., Boubekeur, N., Domingue, F.: Microwave sensing schemes of CPW resonators fully printed on humidity sensitive substrates. *IEEE Microw. Wirel. Compon. Lett.* **29**(4), 303–305 (2019)

5 Lai, N.D., Zheng, D., Jelezko, F., Treussart, F., Roch, J.F.: Influence of a static magnetic field on the photoluminescence of an ensemble of nitrogen-vacancy color centers in a diamond single-crystal. *Appl. Phys. Lett.* **95**(13), (2009) Art. no. 133101

6 Mrózek, M., Mlynarczyk, J., Rudnicki, D.S., Gawlik, W.: Circularly polarized microwaves for magnetic resonance study in the GHz range: Application to nitrogen-vacancy in diamonds. *Appl. Phys. Lett.* **107**(1), (2015) Art. no. 013505.

7 Yuan, H. et al.: Frequency-tunable and circularly polarized microwave resonator for magnetic sensing with NV ensembles in diamond. *IEEE Sensors J.* **20**(15), 8477–8482 (2020)

8 Bayat, K., Choy, J., Farrokh Baroughi, M., Meesala, S., Loncar, M.: Efficient, uniform, and large area microwave magnetic coupling to NV centers in diamond using double split-ring resonators. *Nano Letters*. **14**(3), 1208–1213 (2014)

9 Hu, H., Chen, F., Chu, Q.: A compact directional slot antenna and its application in MIMO array. *IEEE Trans. Antenn. Propag.* **64**(12), 5513–5517 (2016)

10 Ibrahim, M.I., Foy, C., Englund, D.R., Han, R.: High-scalability CMOS quantum magnetometer with spin-state excitation and detection of diamond color centers. *IEEE J. Solid-State Circuits*. **56**(3), 1001–1014 (2021)

11 Gao, Y. et al.: Diamond NV centers based quantum sensor using a VCO integrated with filtering Antenna. *IEEE Trans. Instrum. Meas.* **71**, 1–12 (2022). Art no. 2005112.